RENATA BELISÁRIO

INFECTION BY *Neopestalotiopsis* spp. OCCURS ON UNWOUNDED EUCALYPTUS LEAVES AND IS FAVORED BY LONG PERIODS OF LEAF WETNESS

Dissertation presented to the Universidade Federal de Viçosa, as part of the Plant Pathology Program requirements in order to obtain the Magister Scientiae degree.

VIÇOSA
MINAS GERAIS – BRAZIL
2018

T

Belisário, Renata, 1993-
B431i Infection by *Neopestalotiopsis* spp. occurs on unwounded
2018 eucalyptus leaves and is favored by long periods of leaf wetness /
Renata Belisário. - Viçosa, MG, 2018.
ix, 43 f. : il. (algumas color.) ; 29 cm.

Inclui anexos.
Orientador: Gleiber Quintão Furtado.
Dissertação (mestrado) - Universidade Federal de Viçosa.
Referências bibliográficas: f. 24-31.

1. *Neopestalotiopsis. 2.* Eucalipto. 3. Florestas. 4. Produtividade.
5. Eucalipo - Propagação in vitro. 6. Fungos. 7. Ascomicetos.
8. Florestas - Doenças e pragas. I. Universidade Federal de Viçosa.
Departamento de Fitopatologia. Mestrado em Fitopatologia. II. Título.

CDD 22. ed. 632.36

RENATA BELISÁRIO

INFECTION BY *Neopestalotiopsis* spp. OCCURS ON UNWOUNDED EUCALYPTUS LEAVES AND IS FAVORED BY LONG PERIODS OF LEAF WETNESS

Dissertation presented to the Universidade Federal de Viçosa, as part of the Plant Pathology Program requirements in order to obtain the *Magister Scientiae* degree.

APPROVED: July 23rd, 2018.

Lúcio Mauro da Silva Guimarães

Danilo Batista Pinho

Lucas Magalhães Abreu

Gleiber Quintão Furtado
(advisor)

I am nothing.
I will always be nothing.
I cannot want to be something.
But I have in me all the dreams of the world.

Fernando Pessoa, TABACARIA

To my parents for guidance, support, and unconditional love,
I dedicate this dissertation

ACKNOWLEDGEMENTS

Firstly, I would like to express my deep gratitude to my parents, Paola A. R. Belisário and Marcelo A. Belisário for believing me and supporting me in every decision.

I would also like to thank my sister Bárbara Belisário for her advices and great company even through our ups and downs.

Moreover, I wish to express my sincere acknowledges:

To my dear family, especially my supportive grandma Dilma; my cousins Ana, Lorena, Carolina, Marina, Cecília, Guilherme, Arthur, and André; my aunts Kátia, Cláudia Carlota, Cláudia Brandão, and Meire; and my uncles Beto and Heraldo.

To Davi, for his patience and caring, for encouraging me to grow personally and professionally.

To my long-time friends (siblings), especially Marina Cabizuca, Yago Rocha, Júlia Menicucci, and Thaís Martins for all their strenght, motivation, and for sharing the most wonderful moments with me. To my friends, Bárbara Azevedo, Jessica Cunha, Fernanda Souza, Lívia Torres, and Natasha Areco for all the support and for keeping me happy.

To my roommates Débora Muratori, Bruna Vilela, and Diana Posada, for the unforgettable moments and for our get-together times after work.

To my dear dog Frido, who really understands my emotions and cheers me by offering a comforting paw.

To Fatinha and Enemir, my unforgettable professors who always inspire me.

To Professor Gleiber Quintão Furtado for being a great supervisor and friend. I am thankful for his aspiring guidance, invaluably constructive criticism, and advices during the research work.

To my Viçosa family (panelinha): Flávia Rodrigues, Luísa Borges, and Marcela Uli, for their joy, support, and friendship.

To the friends from the Forest Pathology laboratory for their help and funny moments. To Dr. Carlos Eduardo Aucique-Pèrez, who provided insights and expertise that greatly assisted this research.

To the GEAFIP study group, for giving me the opportunity to learn with them in a pleasant environment.

To the Department professors, particularly Dr. Fabrício de Ávila Rodrigues, Dr. Robert Weingart Barreto, and Dr. Lucas Magalhães Abreu, who assisted my projects and taught me important lessons.

To all staff of the Laboratory of Mycology and Etiology of Fungal Plant Diseases and the Plant Diseases Clinic. Without their precious suggestions and assistance, it would not be possible to conduct this research.

To the Nucleus of Microscopy and Microanalysis from the Universidade Federal de Viçosa for providing the equipment and technical support for experiments involving scanning electron microscopy, especially Carlota Coelho Barroca.

To CENIBRA and all its staff, especially Alex de Barros Medeiros and João Batista Senra, for taking keen interest on our project work, for welcoming our lab team to the company, and for providing the plants used in the experiments.

To the University employers for the rendered services.

To the Universidade Federal de Viçosa and the Plant Pathology Program for the quality of education.

To the Conselho Nacional de Desenvolvimento Científico e Tecnológico (CNPq) for the financial support and scholarship concession.

To all that I forgot to mention, but are certainly important to me, thank you.

BIOGRAFY

RENATA BELISÁRIO, daughter of Paola Amanda Rosa Belisário and Marcelo Antônio Belisário, was born in March 4th of 1993 in Belo Horizonte, Minas Gerais, Brazil. She concluded her undergraduate education in Biological Sciences in 2015 (bachelor's degree) and 2016 (licentiate's degree) at the Pontifícia Universidade Católica de Minas Gerais, Belo Horizonte, Brazil. Part of her undergraduate studies was done in Peterborough, Canada, between 2014 and 2015, through an exchange program funded by the Government of Brazil. Since 2016, her academic activities have been supervised by Professor Gleiber Quintão Furtado at the Forest Pathology Laboratory – Department of Plant Pathology. Renata obtained her Magister Scientiae degree in Plant Pathology at the Universidade Federal de Viçosa in 2018.

SUMMARY

ABSTRACT

BELISÁRIO, Renata, M.Sc., Universidade Federal de Viçosa, July, 2018. **Infection by Neopestalotiopsis spp. occurs on unwounded eucalyptus leaves and is favored by long periods of leaf wetness.** Advisor: Gleiber Quintão Furtado.

Brazil is the leader in the global ranking of forest productivity; however, one of the major challenges to eucalyptus production is the existence of fungal diseases. A severe epidemic caused by pestalotiopsis-like fungi was continuously observed in a forest nursery in Brazil, causing a huge impact on the eucalyptus micropropagation stages. The aims of the present study were (i) to identify the causal agent associated with pestalotiopsis leaf spot and dieback in eucalyptus; (ii) to assess the pathogenicity of the isolates to different commercial clones; (iii) to evaluate the wetness conditions that were favorable for both conidial germination and infection by the pathogen; (iv) to evaluate if pestalotioid fungi obtained from different host species could infect eucalyptus; and (v) to elucidate the fungal penetration process on eucalyptus leaves. Results showed that Neopestalotiopsis spp. are capable of causing symptoms on unwounded eucalyptus leaves and that disease development strongly requires specific environmental conditions. Therefore, our data demonstrate that long leaf wetness periods ($\geq$ 72 h) were required to establish successful host–fungus relationships, causing expanded lesions to eucalyptus seedlings. Moreover, conidia germinated within 6 hours after inoculation and there was a tendency of direct germ tube penetration on host leaf tissues to reach a suitable infection. All of the four commercial clones tested were susceptible to the pathogen and the set of data disputes the assumption that pestalotioid fungi are weak and opportunistic. Our data imply that single-gene phylogenetic trees constructed from ITS and TEF regions showed unresolved polytomies (multifurcating branches) and poor resolution. Only TUB and multi-locus phylogenies were stable and provided sufficient resolution tree topologies. This is the first report of different phylogenetic species of Neopestalotiopsis causing dieback, leaf and stem lesions in eucalyptus seedlings. Considering the importance of this pathogen on aerial parts of eucalyptus, comprehension of the favorable conditions required for disease progress may provide a basis for developing novel management strategies in forest nurseries.

RESUMO

BELISÁRIO, Renata, M.Sc., Universidade Federal de Viçosa, julho de 2018. **A infecção de Neopestalotiopsis spp. ocorre em folhas de eucalipto sem ferimento e é favorecida por longos períodos de molhamento foliar.** Orientador: Gleiber Quintão Furtado.

O Brasil lidera o ranking global de produtividade florestal; todavia, um dos maiores desafios à produção de eucalipto é a ocorrência de doenças em viveiros. Uma epidemia severa causada por fungos pestalotiopsis-like foi continuamente observada em um viveiro florestal no Brasil, causando impacto negativo nas etapas de micropropagação de eucalipto. Os objetivos do presente estudo foram (i) identificar o agente causal associado à mancha de pestalotiopsis e morte descendente em eucalipto; (ii) determinar a patogenicidade dos isolados para diferentes clones comerciais; (iii) avaliar as condições de umidade favoráveis para a germinação dos conídios e para a infecção pelo patógeno; (iv) avaliar se fungos pestalotioides obtidos de diferentes espécies hospedeiras são capazes de infectar eucalipto; e (v) elucidar o processo de penetração do fungo nas folhas de eucalipto. O conjunto de resultados mostrou de forma pioneira que espécies de Neopestalotiopsis são capazes de causar lesões expandidas em folhas de eucalipto na ausência de ferimento e sob período constante de molhamento foliar (≥ 72 h). Estas condições ambientais são favorecidas pelo sistema de propagação clonal de eucalipto. Além disso, verificou-se que Neopestalotiopsis germinou a partir de 6 horas após a inoculação, havendo uma tendência de penetração direta nas células epidérmicas do hospedeiro. Todos os clones testados foram suscetíveis ao patógeno, portanto contesta-se a premissa de que os fungos pestalotioides são patógenos secundários. Filogeneticamente, os dados sugerem que as árvores individuais para as regiões gênicas ITS e TEF apresentaram muitas politomias e baixa resolução. Apenas as árvores construídas para TUB e a topologia consenso usando três loci foram estáveis e apresentaram alto suporte para os ramos. Este é o primeiro relato de diferentes espécies filogenéticas de Neopestalotiopsis causadoras de seca de ponteiros, lesões foliares e de hastes em mudas de eucalipto. Por conseguinte, o conhecimento gerado a partir do presente estudo pode fornecer informações úteis para o desenvolvimento de novas estratégias de manejo em viveiros florestais.

1. INTRODUCTION

Brazil is the leader in the global ranking of forest productivity, reaching approximately 35.7 m^3 / ha.yr for eucalyptus plantations (Ibá, 2017). Furthermore, capital expenditure on that crop accounts for approximately 75% of the total in relation to other woody plants (ABRAF, 2013). Due to edaphoclimatic conditions, the availability of land, and the cutting-edge technology developed by national companies, Brazil is able to supply commodities that meet international demand (Ibá, 2017).

The genus Eucalyptus belongs to the Myrtaceae family and comprises more than 700 botanical species originating in Australia and Tasmania. The physical and chemical properties make it economically important in several sectors, such as the wood industry, production of timber and pulp, pharmaceutical industry, fragrance market, fuelwood, and extractive industries (ANPSA, 2017).

However, one of the major challenges to eucalyptus seedling production is the occurrence of fungal diseases, such as leaf spot, gray mold, rust, cutting rot, and damping-off (Brown et al., 2000; Ferreira, 1989). For instance, economic problems were reported on eucalyptus nurseries and they might be associated with high relative humidity followed by long periods of leaf wetting. These are conditions required in this plant production system (Zaldúa and Sanfuentes, 2010).

Between 2017 and 2018, a severe epidemic caused by pestalotiopsis-like fungi was continuously observed in a forestry company in Brazil. In the shade house, dark-brown to black lesions were observed along the main leaf veins and stems of the mini-cuttings, whereas masses of black conidiomata developed on the surface of the lesions.

In the clonal garden, micro-stumps exhibited symptoms of dieback which progressed to the death of plants.

To date, only four species of Neopestalotiopsis (N. australis, N. eucalypticola, N. mesopotamica, and N. steyaertii) and six species of Pestalotiopsis (P. colombiensis, P. disseminata, P. funereoides, P. mangiferae, P. microspora, and P. neglecta) were previously described in association with Eucalyptus spp. (Maharachchikumbura et al., 2016; Mittal et al., 1990; Yuan and Mohammed, 1997). Indeed, little is known about the importance of pestalotiopsis leaf spot in forest nurseries in Brazil. This disease is commonly attributed to opportunistic or fungi which infect physiologically weakened eucalyptus plants (Alfenas et al., 2009). Moreover, some species were also considered weak and secondary pathogens in certain crops (Coyier and Roane 1986; Madar et al., 1991; Pirone, 1978).

Pestalotiopsis-like members were reported as endophytes (Watanabe et al., 2010), plant pathogenic (Maharachchikumbura et al., 2012), or saprobes (Hu et al., 2007). Furthermore, they can cause several diseases, including canker lesions, dry flower disease, leaf spots, twig dieback, grey blight, tip blight, scabby canker, chlorotic spots, as well as post-harvest diseases (Akinsanmi et al., 2017; Das et al., 2010; El-Argawy, 2015; Espinoza et al., 2008; Rosado et al., 2015; Tagne and Mathur, 2001).

Some researchers separate pestalotiopsis-like species based on host association and conidial characteristics (Maharachchikumbura et al., 2011). However, naming pestalotioid fungi using solely these criteria might be inaccurate because species are not host-specific and they may vary in morphological manners when grown in artificial culture (Sutton, 1980).

Most of the taxa described in the literature are likely to be based on misinterpretations or synonyms of species with broad host ranges (Jeewon et al., 2004; Maharachchikumbura et al., 2011). In addition, taxonomy presents a challenging situation since there are few distinct species and many sequences of Pestalotiopsis deposited in GenBank are not linked to any type material (Maharachchikumbura et al., 2011). Therefore, those gene sequences do not accurately clarify species names unless they are derived from ex-types (Maharachchikumbura et al., 2016).

Based on a phylogenetic analysis of the large subunit (LSU) of the nuclear ribosomal RNA (rRNA) dataset, the above-mentioned genus was segregated into three genera: Pestalotiopsis, Neopestalotiopsis, and Pseudopestalotiopsis. Pestalotiopsis members are morphologically characterized by their five-celled, fusiform conidia, with hyaline end cells and three light concolorous median cells. Neopestalotiopsis can be distinguished from Pestalotiopsis by its versicolorous median cells. Pseudopestalotiopsis members, in turn, have concolorous median cells and its lineage clustered as a basal sister clade to Neopestalotiopsis (Maharachchikumbura et al., 2016).

There is still no information on Pestalotiopsidaceae members causing diseases on eucalyptus seedlings worldwide. Therefore, the aims of the present study were **(i)** to identify the causal agent associated with pestalotiopsis leaf spot and dieback in eucalyptus; **(ii)** to assess the pathogenicity of the isolates to eucalyptus clones; **(iii)** to evaluate the temperature and wetness conditions that were favorable for conidial germination; **(iv)** to determine if leaf wetness facilitates the infection by the pathogen; **(v)** to evaluate if pestalotioid fungi obtained from different host species could infect eucalyptus; and **(vi)** to elucidate the fungal penetration process on eucalyptus leaves.

2. MATERIALS AND METHODS

2.1 Fungal isolates and preservation of the cultures

Symptomatic mini-cuttings and micro-stumps of a hybrid clone of eucalyptus (CNB 019 - Eucalyptus grandis×Eucalyptus urophylla) were randomly collected in two seasons from clonal gardens at the Celulose Nipo-Brasileira (CENIBRA) company, Minas Gerais state, Brazil. Five micro-stumps and three mini-cuttings were first examined under a stereomicroscope [Motic® SMZ-140 (20X)] for observation of fungal structures. All eight samples were representative of the disease and showed standard symptoms of both pestalotiopsis leaf spot and dieback.

For isolation purposes, a mass of conidia was transferred, under aseptic conditions, from symptomatic plants to Petri dishes containing potato dextrose agar (PDA-Acumedia®). Surface disinfection of the fragments was done by stepwise washing in 70% ethanol for 30 seconds and 2% sodium hypochlorite solution for two minutes. The plates were incubated at 25ºC with a 12-hour photoperiod, for 15 days or until growth and sporulation were observed.

Single conidia cultures were obtained on PDA and preserved in sterile saline solution, glycerol (15%) and silica gel (Zauza et al., 2007). The dried material was deposited in the Herbarium at the Universidade Federal de Viçosa (UFV), Brazil. The preserved isolates were deposited in the Octavio de Almeida Drumond Collection (COAD) at UFV, Brazil.

2.2 DNA extraction and amplification

Eight single-spore isolates were grown on PDA at 25°C under a 12-hour photoperiod for seven days. Mycelium was scraped off with a sterilized wooden toothpick

and transferred to a 1.5 mL microcentrifuge tube. The extraction was performed by mechanical disruption using stainless steel beads. Total DNA was extracted using the Wizard® Genomic DNA Purification Kit (Promega Corporation, WI, EUA) following the protocol described by Pinho et al. (2013).

The primer pairs ITS5 + ITS4 (White et al., 1990), EF1-728F (Carbone and Kohn, 1999) + EF-2 (O'Donnell et al., 1998), and T1 (O'Donnell and Cigelnik, 1997) + Bt2b (Glass and Donaldson, 1995), were used to amplify the ITS, EF-1α, and β-tub genes, respectively. PCR was performed with 6 μL of Dream Taq TM PCR Master Mix 2× (MBI Fermentas, Vilnius, Lithuania); 0.5 μL of 10 μM each forward and reverse primer; 0.5 μL of dimethyl sulfoxide (DMSO, Sigma–Aldrich, St. Louis, MO); 1 μL of 100× (10 mg/mL) Bovine Serum Albumin (BSA, Sigma–Aldrich,); 1 μL of genomic DNA (25 ng/μL) and 2.5 μL of nuclease-free water.

Amplification was performed with an initial denaturing step at 94°C for 5 min, followed by 38 cycles of denaturation at 94°C for 30 sec, annealing at 54°C for 30 sec (EF-1α and β-tub), or 60°C for 30 sec (ITS), extension initial 72°C for 45 sec, and final extension at 72°C for 7 min. The presence of PCR products was confirmed by 2% agarose gel electrophoresis.

The amplicons were purified with ExoSAP-IT™ PCR Product Cleanup Reagent; quantified using a NanoDrop instrument (Thermo Fisher Scientific, Waltham, MA, USA); and subjected to Sanger sequencing by Myleus Biotecnologia, Brazil (http://facility.myleus.com/).

2.3 Data editing and phylogenetic analyses

The nucleotide sequences were edited and checked manually with SeqAssem software (Hepperle, 2004). Nucleotide arrangements with ambiguous positions were clarified by analyzing the sequences obtained with both primers (forward and reverse).

A BLAST search was performed to check for similarity with other sequences available at the GenBank's database. The closest hit sequences (Table 1) were aligned with the multiple sequence alignment program ClustalW (Larkin et al., 2007) implemented by MEGA 7 (Kumar et al., 2016). Manual adjustments were made when necessary.

Substitution models were determined separately for each gene partition using jModelTest 2.1.10 (Darriba et al., 2012), in which they were selected according to the Akaike Information Criterion (AIC).

Bayesian Inference (BI) trees were generated employing the Markov Chain Monte Carlo (MCMC) algorithm. The phylogenetic analyses were performed through CIPRES Science Gateway (Miller et al., 2010) using MrBayes 3.2.6 on XSEDE tool (Ronquist and Huelsenbeck, 2003). Four MCMC chains were run simultaneously from random trees for ten million generations and sampled every 1,000 generations. The first 2,500 trees were discarded as the burn-in phase of each analysis. The posterior probabilities were determined from the remaining trees. The phylogenetic trees, rooted with Pseudopestalotiopsis theae MFLUCC 12-0055, were visualized in the FigTree software program (Rambaut, 2009). The trees obtained from single genes and multi-locus alignments were compared along with their performance in species recognition.

Additionally, Maximum Likelihood (ML) analyses were generated for each separate gene and multi-locus alignment using MEGA 7. ML trees were inferred based

on the Nearest-Neighbor-Interchange (NNI) heuristic method and the Tamura-Nei Substitution model. The chain robustness was assessed through the bootstrap re-sampling strategy with 10,000 bootstrap test replicates. The trees were visualized using the FigTree software program. Pseudopestalotiopsis theae MFLUCC 12-0055 was used as the outgroup.

The resulting tree topologies using the two methods (BI and ML) were then compared and the phylogram layout was edited with CorelDRAW Graphics Suite 2018 (https://www.coreldraw.com/br/).

2.4 Morphological characterization

Morphological characterization was made for isolates obtained from lesions on eucalyptus seedlings. Fungal characters (conidia and appendage sizes, number of apical appendages) were measured with 30 replicates for each structure. Colony color on PDA was determined on the basis of a mycological color chart (Rayner, 1970).

To obtain slide cultures, a small fragment of PDA culture medium was placed on a sterile glass slide. The slide was suspended on glass rods in a Petri dish containing moistened filter paper. Fragments of each isolate's mycelium were transferred to the four edges of the culture medium and covered with a coverslip. Petri dishes containing slides were incubated at 25ºC with a 12-hour photoperiod. After five days, the coverslip was removed and placed on a glass slide. Images of fungal structures were taken by using an Olympus BX 53 compound microscope fitted with a digital camera (Olympus Q-COLOR5).

For mycelial growth rate determination, a disk of approximately 1 cm in diameter was transferred to three different culture media: PDA, synthetic nutrient-poor agar

(SNA), and malt extract agar (MEA) (Zauza et al., 2007). Cultures were incubated as previously mentioned and evaluation was carried out every two days by measuring the colonies diameter, obtained by the average of two diametrically opposed measurements. It was assessed until the control group reached the edge of the Petri dish (Oliveira, 1991). The experiment was carried out twice in a completely randomized design with eight replicates, each one comprising a Petri dish (Ø = 90 mm). The growth rate was then calculated as the area under the curve (AUC) considering that the colonies grew in a circular regular manner. Analysis of variance (ANOVA) was run to compare the means using the MiniTab 17 Statistical Software (www.minitab.com).

2.5 Pathogenicity tests of Neopestalotiopsis spp. on commercial eucalyptus clones

In order to evaluate Neopestalotiopsis spp. pathogenicity to commercial eucalyptus clones, four genotypes Eucalyptus grandis×Eucalyptus urophylla (CNB 019, CNB 021, CNB 029, and CNB 030) were selected for inoculation trials, using 2-month-old plants.

Mycelium plugs taken from the edges of actively growing isolates (COAD 2392, COAD 2393, COAD 2394, and COAD 2395) were placed onto ten wounded (five seedlings) and ten unwounded leaves (five seedlings) of each genotype. For the control treatment, five plants with wounded and unwounded leaves were inoculated with sterile PDA disks. In order to reduce desiccation of the inoculum, sterile distilled water (SDW) was sprayed over the plants before and after inoculation. Plants were kept for seven days in a mist irrigation chamber at 25°C with photoperiod (225 μE m^{-2} s^{-1}) adjusted to 12 hours. Trials were repeated twice over time. The pathogens were re-isolated from

inoculated plant tissues and the cultures were compared with the original strains, confirming Koch's postulates.

Incidence for infected leaves were analyzed with ExpDes package (Ferreira et al., 2014) of R software (R Development Core Team) in a completely randomized design, forming a 2 × 4 × 4 factorial (two inoculation methods, four clones, and four isolates). Data were statistically examined using ANOVA and tested for significant ($P \leq 0.05$) clone, isolate, and inoculation method differences using Tukey's and F-tests.

2.6 Effect of wetness period on the development of pestalotiopsis leaf spot

Each sporulating colony incubated for ten days was washed with SDW and the conidial suspension was transferred to a beaker containing one drop of Tween 80 (0.05% v/v). The suspension was filtered through one layer of gauze over a sieve large enough not to retain the spores. Spore density was then adjusted to 2×10^5 conidia/mL, following Neubauer chamber counts.

For each of isolate, 40 eucalyptus seedlings (CNB 019) were spray inoculated without superficial injury to evaluate the disease progress. Then, plants were conditioned in a mist irrigation chamber at 25°C with photoperiod (225 μE m^{-2} s^{-1}) adjusted to 12 hours. After 24, 48, and 72 hai, ten seedlings for each different time were subsequently transferred to a growth chamber (28 ± 2ºC, 80 ± 5% humidity, 12-hour photoperiod). Other ten plants were kept in the mist irrigation chamber for seven days (168 hai). Five control seedlings were sprayed with SDW only and maintained in the same conditions. Evaluations were carried out daily until the onset of symptoms and signs. They were recorded with a Nikon Coolpix P510 digital camera. Experiments were conducted three times.

2.7 Cross-inoculation tests

In order to test alternative hosts of Neopestalotiopsis spp., isolates obtained from seven different species of Myrtaceae and Arecaceae (Table 2) were inoculated on 2-month-old eucalyptus seedlings. Isolates were kindly donated by the Laboratory of Mycology and Etiology of Fungal Plant Diseases and the Forest Pathology Laboratory, both located at UFV, Brazil.

Mycelial plugs of the same size (4 mm diameter) were taken from the edges of actively growing fungal colonies on PDA and placed over the surface leaves with mycelium facing the cambium. For each isolate, disks were placed onto 20 wounded and 20 unwounded leaves in each of three eucalyptus seedlings (CNB 019). On control treatment, only PDA plugs without fungal culture were placed onto wounded and unwounded leaves. Plants were kept for 48 hours in a mist irrigation chamber at 25°C with photoperiod (225 μE m^{-2} s^{-1}) adjusted to 12 hours and subsequently maintained in a growth chamber (28 ± 2ºC, 80 ± 5% humidity, 12-hour photoperiod). Then, fungal isolates were recovered from the lesion margins, confirming Koch's postulates. Experiments were conducted twice over time.

2.8 Effect of temperature and wetness periods on conidial germination under in vitro conditions

In order to test the effects of wetness periods and temperature on spore germination, three droplets (30 μL) of a conidial suspension adjusted to 10^5 conidia/mL were deposited onto polystyrene Petri dishes. Plates were placed into sealed boxes containing 60 mL of SDW each to maintain a constant level of free water. Dishes distributed in two replicates for each temperature were incubated in the dark in five

different temperatures: 15, 20, 25, 30, and 35°C. Continuous wetting periods consisted of 1, 3, 6, 9, 12, 24, 48, and 72 hours. Wetness treatments were halted by depositing 10 μL of lactoglycerol on each droplet and coverslips were placed over the drops before assessing the percentage of spore germination. It was evaluated by determining the number of germinated conidia out of 100 per replicate. Conidia were recorded as having germinated when the length of the germ-tube was greater than its width under a light microscope at a 400× magnification. The experiment was carried out twice and each replication consisted of a Petri dish containing three droplets of the spore suspension. The relationship of temperature and wetness on germination was described through a response surface model under SigmaPlot 11 (http://www.sigmaplot.co.uk).

2.9 Assessing fungal penetration through Scanning Electron Microscopy (SEM)

The most virulent isolate (COAD 2393) obtained from leaves of the most susceptible eucalyptus clone (CNB 019) was incubated in a growth chamber at 25°C with a 12-hour photoperiod for seven days.

Leaves were randomly detached from the first two pairs of eucalyptus seedlings, washed in SDW, air dried and kept in sterilized trays. Then, plastic trays were moistened with 200 mL of SDW to create a saturated environment. The sporulating colony was washed with SDW and the conidial suspension was used for inoculation. Three spore suspension droplets of 25 μL were deposited onto leaves in replicates. The boxes were covered with plastic bags and incubated at 25°C with a 12-hour photoperiod for 24 hours. After that, samples were collected after 3, 6, and 24 hai. Fragments were then placed onto wells of porcelain spot plates within small plastic boxes, which were lined with one sheet

of moistened paper. Samples were fixed for 12 hours in osmium vapor according to Kitajima and Leite (1999). After fixation, they were dehydrated for 24 hours in hermetically sealed containers containing silica gel. These samples were mounted on aluminum stubs with a double-coated carbon tape and were sputter-coated with gold (Balzers Union, model FDU 010). Infection process was observed and photographed with a LEO scanning electron microscope (SEM) (model 1430 VP), coupled with energy-dispersive x-ray spectrometer, operating at 10 kV with a working distance ranging from 10 to 30 mm.

3. RESULTS

3.1 Fungal isolates and material preservation

Eight pestalotioid-fungal isolates were obtained from symptomatic eucalyptus micro-stumps and mini-cuttings stems and leaves (Fig. 1a, b). Dried specimens of Neopestalotiopsis spp. were deposited in the Herbarium at the public institution UFV under the codes VIC 44459, VIC 44460, VIC 44461, VIC 44462, VIC 44463, VIC 44464, VIC 44465, and VIC 44466. The preserved isolates were deposited in COAD culture collection, at the same institution, under the codes COAD 2392, COAD 2393, COAD 2394, COAD 2395, COAD 2464, COAD 2465, COAD 2466, and COAD 2467.

3.2 Morphological characterization

Colonies on PDA attained 80-90 mm diam after eight days at 25°C and the mycelial growth rate was calculated as the area under the curve (AUC) considering the time interval from two to eight days. The growth rates for Neopestalotiopsis spp. revealed no significant statistical differences among the three media: PDA (8.52 mm^2/day; $\overline{X}$ AUC

= 237.80[a]), MEA (7.59 mm^2/day; $\overline{X}$ AUC = 230.01[a]), SNA (8.01 mm^2/day; $\overline{X}$ AUC = 228.96[a]), whereas the fastest colony development occurred on PDA. All media tested supported sporulation, except SNA. Colonies generally showed sparse aerial mycelium on the surface and indistinct patterns among isolates, except for the abundance of conidiomata (gregarious to concentric). Cultures were flat, whitish to pale luteous-colored, smooth on the edges (Fig. 1c); reverse was buff in color with dense and black conidiomata, sometimes with distinct zonation (Fig. 1d).

Since isolates obtained in this study generally showed overlapped morphological characters, they were described according to characteristics they had in common. A detailed morphological comparison between the isolates is shown in Table 3.

Conidiomata acervuli semi-immersed to pycnidial, glistening globose, wet, and black conidial masses in culture on PDA. Conidiophores often reduced to conidiogenous cells. Conidiogenous cells hyaline, discrete, short (Fig. 1e). Conidia 4-septate, fusiform to ellipsoid, straight to slightly curved, varying between 18.0 and 24.5 μm in length and between 6.0 and 7.5 μm in width (conidia 21.0–24.0 × 6.0–6.5 μm for isolates COAD 2395, COAD 2464, COAD 2465, and COAD 2466; 18.0–24.5 × 6.0–7.0 μm for isolates COAD 2392 and COAD 2467; and 21.5–24.5 × 6.5–7.5 μm for isolates COAD 2393 and COAD 2394). Basal cell hyaline, conic to obconic with a truncate base; three median cells versicolored, doliiform to cylindrical; apical cell hyaline, cylindric to subcylindric. All isolates showed hyaline basal and apical appendages. The number of apical appendages ranged from two to three, in which three was the most common (Fig. 1e–h, and Fig. 7a, b). Apical appendages were always unbranched and mostly tubular; their length was 8.0 to 22.0 μm (9.5–25.5 μm for isolates COAD 2395, COAD 2464, COAD 2465, and COAD 2466; 12.0−22.0 μm for isolates COAD 2392 and COAD 2467; and 8.0–22.0 μm for

isolates COAD 2393 and COAD 2394), while basal appendage lenght varied between 3.5 and 5.0 µm (3.5–5.0 µm for isolates COAD 2395, COAD 2464, COAD 2465, and COAD 2466; 3.5−4.0 µm for isolates COAD 2392 and COAD 2467; and 3.5–4.0 µm µm for isolates COAD 2393 and COAD 2394). Apical appendages of all isolates arised from the apex of the apical cell (Fig. 1e, f, h), except COAD 2392 which presented apical appendages inserted at different loci in the upper half of the apical cell (Fig. 1g).

3.3 Phylogenetic analyses

Phylogenetic analyses of the 54 isolates representing the known species of Neopestalotiopsis and the outgroup Pseudopestalotiopsis theae were performed on single loci and concatenated datasets (ITS, TEF, and TUB), as shown in Table 1. The alignment comprised 450 characters with gaps for ITS, 481 for TEF, and 635 for TUB. Once the likelihood scores were calculated, the models were selected according to the Akaike Information Criterion (AIC). The best nucleotide substitution models for the Bayesian Inference were HKY+G for ITS, HKY+I+G for TEF, and SYM+I+G for TUB.

Our results demonstrated that individual phylogenetic trees constructed from ITS and TEF regions showed multifurcating branches and poor resolution. For instance, Maharachchikumbura et al. (2014) presented a consensus topology in which N. umbrinospora, N. honoluluana, and N. samarangensis consisted of well-supported separable species; however, in the ITS gene tree of the present study there was a polytomy between them. In addition, BI from TEF sequence data exhibited a huge polytomy including the eight isolates obtained in this work, with weakly supported nodes (bootstrap less than 50% for all the terminal clades; results not shown).

Several clades representing known species on the concatenated gene tree were poorly supported on the single phylogram for ITS and TEF. However, comparing single topologies from both methods (BI and ML), TUB proved to be a favorable taxonomic marker for Neopestalotiopsis in this study.

The multi-locus tree obtained through BI method was the most accurate topology and apparently reflected the natural evolutionary relationships among Neopestalotiopsis spp. The ML tree corroborates with the tree topology of the Bayesian consensus tree, but the first provided lower support values for most branches.

The eight strains were separated into three clades (Fig. 2) and there were close relationships between some reference sequences and isolates in our study. COAD 2393 and COAD 2394 grouped together with high bootstrap confidence (86%) and posterior probability (1.0), being positioned as N. protearum (0.86/95%). The isolates COAD 2464, COAD 2465, COAD 2466, and COAD 2395 clustered together with strong BI support (0.90). The remaining two isolates, COAD 2393 and COAD 2467, were grouped with N. rosae and they are hereby identified as belonging to that species, despite the support values were relatively low (<0.70/<50%).

3.4 Pathogenicity tests of Neopestalotiopsis spp. on commercial eucalyptus clones

All isolates of Neopestalotiopsis were pathogenic to eucalyptus regardless of the inoculation method and wounded seedlings were more susceptible to the pathogen compared to unwounded plants. The disease incidence (% leaves infected) for wounded leaves was statistically different only for the clone CNB 030 inoculated with N. protearum - COAD 2394 (Fig. 3). However, the disease incidence varied among clones

and isolates for unwounded leaves. Between all isolate × clone interactions, isolate COAD 2393 (Neopestalotipsis protearum) was the most aggressive, causing lesions on a larger number of clones irrespective to wounds.

The inoculated seedlings showed dark-brown to black lesions along the main leaf veins and stems within three days for wounded plants and five days for unwounded seedlings. Masses of black conidiomata developed on the surface of the lesions (Fig. 4f) and, in 80% of the seedlings, dieback progressed to the death of plants. The fungus was recovered from inoculated plants, and the colonies obtained exhibited the same pattern observed prior to inoculation, confirming Koch's postulates. Replicates showed the same tendency across treatments. No symptoms of pestalotiopsis leaf spot were observed for control plants (Fig. 4g).

3.5 Effect of wetness period on the development of pestalotiopsis leaf spot

For all isolates tested, the disease development was favored mostly by prolonged humidity. Seedlings kept in a mist irrigation chamber under 24 and 48h and transferred to a growth chamber (28 ± 2ºC, 80 ± 5% humidity, 12-hour photoperiod) remained symptomless compared to the control plants (Fig. 4a, b). Conversely, eucalyptus seedlings incubated for 72h under mist irrigation chamber and transferred to a growth chamber showed disease symptoms seven days after inoculation (dai) only on the first two pairs of leaves (Fig. 4c). When the seedlings inoculated by aspersion were subjected to 168h of continuous wetness, dieback progressed to the death of all plants over the time (Fig. 4d, e). Therefore, longer wetness periods were required to produce broader disease levels.

3.6 Cross-inoculation tests

The potential infection of isolates obtained from different hosts was investigated on eucalyptus seedlings. All isolates of Neopestalotiopsis spp. were pathogenic to 100% of the tested plants (Fig. 5). Leaf-wounding prior to inoculation was not necessary for disease development regardless of the host. Nonetheless, symptom development was enhanced provided that foliage was subjected to injuries. The common symptom of infection was leaf spot five days after inoculation for wounded leaves and seven days for unwounded leaves. The Neopestalotiopsis species showed variation in virulence, with the isolates originating in Wodyetia bifurcata, Caryota mitis, and Dypsis lutescens causing more expanded lesions than those collected from other host species. Elseways, control plants remained symptomless (Fig. 5i).

3.7 Effect of temperature and wetness periods on conidial germination under in vitro conditions

In spite of a relationship between temperature and wetness ($p \leq 0.001$), analysis of combined data suggested that spore germination was stronger influenced by long exposure to conidial saturation with SDW (Fig. 6). There was an exponential increase in germination rate between 3 and 12h of wetness, whilst longer wetting periods led to a plateau (85–95%) regardless of the temperature. Optimum conidial germination was observed at 30°C, with germ-tube development starting within 3h and 99% conidia germination attained within 24h. In some cases, appressoria-like were observed after 9h under controlled environmental conditions. Replicates showed the same tendency across treatments.

3.8 Assessing fungal penetration through Scanning Electron Microscopy (SEM)

The micrographs showed germinating conidia emitting a single germ tube from the second pigmented median cell. At 3 hai, Neopestalotiopsis prepared the site infection probably by secreting enzymes that degraded the wax layer (Fig. 7a). At 6 hai, conidia produced long germ tubes and attempted to directly penetrate the epidermis of the adaxial surface without any evidence of appressorial formation nor stomatal penetration (Fig. 7c).

4. DISCUSSION

The present study represents the first to elucidate Neopestalotiopsis spp. infection on eucalyptus in Brazil. Results obtained from DNA sequences, morphological characterization, fungal penetration process, cross-inoculation, and pathogenicity tests were analyzed together in order to understand the novel Neopestalotiopsis-Eucalyptus interaction to a forest nursery setting.

For a long time, Pestalotiopsis spp. and allied genera were formerly regarded as weak, opportunistic and secondary pathogens to certain crops (Coyier and Roane 1986; Madar et al., 1991; Pirone, 1978). Nevertheless, Maharachchikumbura et al. (2012) stated that pestalotiopsis-like taxa are important as widespread phytopathogens and this study provides evidence that Neopestalotiopsis spp. is capable of causing leaf spot disease on eucalyptus seedlings. Pestalotiopsis and Neopestalotiopsis species were previously reported to infect only wounded or stressed plants (Keith et al., 2006). For instance, experiments with P. sydowiana in nurseries showed that physical damage to the foliage of ornamental cuttings was necessary to induce pathogenicity (Hopkins and McQuilken,

2000). In contrast, our results proved that Neopestalotipsis spp. were significantly virulent even to unwounded seedlings inoculated by foliar aspersion.

Our data demonstrate that long wetness periods (≥ 72 h) were required to establish successful host–fungus relationships, causing lesions mainly on the first pairs of eucalyptus leaves. Similar results showed that 72-hour foliage wetting was associated with the highest area under the disease progress curve (AUDPC) to cercospora leaf spot on Toona ciliata leaves (Silva et al., 2018). In addition, according to Elmer and Ferrandino (1995), the increased susceptibility in young leaves is explained by the lack of defense-related mechanisms and due to the exposure to abiotic conditions that were propitious for disease development.

In fact, several diseases influenced by sources of splashed water are well documented in the literature. According to Gilet and Bourouiba (2015), this common scenario in forest nurseries provides a significant horizontal velocity to the water droplets, which become a relevant factor in spore dispersal to neighboring seedlings. Moreover, we assume that leaf wetness periods higher than 72 hai are necessary for Neopestalotiopsis to gain stability and assess plant tissues. We believe that the microclimate change on the phylloplane surface (plants subjected to leaf wetness period < 72 h and transferred to the growth chamber at 28 ± 2ºC, 80 ± 5% humidity) has disfavored the entry of the pathogen into the cytoplasm of the host. The lack of information in the literature regarding the infection process raises questions about the pathogen's colonization and its development inside the host.

Since natural openings such as stomata respond to environmental conditions, pathogens can benefit from high humidity and/or release virulence factors to suppress stomatal closure (Zeng et al., 2010). However, in this study, there was no evidence of

stomatal penetration, similar to the results for P. longisetula on strawberry leaves (Rodrigues et al., 2014). Instead, conidia tend to directly penetrate the epidermis to reach a suitable infection. Similarly, Pestalotiopsis malicola produced germ tubes that directly penetrated the cuticle (Gevens et al., 2001). These authors also indicated that a strong initial conidial adhesion occurs at the appendages due to the release of extracellular matrix (ECM) by conidia. This phenomenon may explain the presence of a sturdy adhesion of Neopestalotiopsis spp. to eucalyptus leaves at 3 hai in this study.

Tests involving the effect of foliage wetting period on disease progress were corroborated by in vitro assays, in which Neopestalotiopsis was favored by long periods of wetting. There was an exponential increase in germination rate between 3 and 12h of wetness, whilst longer moist periods led to a plateau (85–95%) regardless of the temperature. Schuh (1991) also found no difference in conidial germination between 15 and 35°C, but prolonged humidity had a strong effect on germination, in agreement with the results presented in this study. Likewise, as stated by Carroll and Wilcox (2003), there was a consistent epidemiological relationship between humidity level and conidial germination. Huber and Gillespie (1992) provided a clear-cut explanation regarding the influence of leaf wetness on epidemiological episodes of fungal diseases, in which short wetting periods restrict conidial germination. Free water on leaf epidermis is required for long enough periods as the germination process starts, otherwise, germ tube growth is negatively affected and infection does not succeed. To some extent, moisture duration is also related to the colonization process, in which lower transpiration is favored by wetness, hence providing higher availability of internal water for the pathogen (Katerji et al., 1986). In this study, the pathogen was able to produce germ tubes within twelve hours and penetrate the host epidermis 24h after inoculation; however, the induction of

symptoms was triggered by continuous foliage wetness since the fungus requires at least 72h to establish successfully in eucalyptus seedlings.

The isolates were used to screen different clones of eucalyptus for susceptibility to infection under greenhouse conditions. All of them were pathogenic and plants shared a similar pattern of signs and symptoms: dark-brown to black lesions along the main leaf veins and stems. However, the disease incidence varied across the tested hybrid clones and isolates mainly for unwounded leaves. This is consistent with Chen et al. (2013), who proved there were differences in Ceratocystis-eucalyptus interaction responses of different genotypes after inoculation. Since all the clones in this study were highly susceptible to at least one isolate, it might be feasible to develop biological control programs and implement phytosanitary management strategies to halt that disease outbreak.

Despite the fact that some pestalotioid-fungi taxa have been recorded solely on one host does not imply that they are host-specific (Jeewon et al., 2004). In this study, cross-inoculation tests demonstrated that pathogenic isolates originally obtained from different hosts caused successful infection on all eucalyptus seedlings tested, regardless of the presence of mechanical injuries. Thus, the present work fully supports the conclusion that several species, as well as multiple isolates of the same species, can occur on an individual host.

Maharachchikumbura et al. (2012) affirmed that phylogenetic species delimitation in Pestalotiopsis should be based on the combined ITS, TEF, and TUB gene regions. Nevertheless, a previous study demonstrated that overall branch-lengths of multi-locus topologies were notably short and the support values were relatively low (Liu et al., 2017). Even though Hyde et al. (2014) and Lazarotto et al. (2014) stated respectively that TEF

and ITS gene regions resolved lineages within Pestalotiopsis, only TUB proved to be a favorable taxonomic marker for Neopestalotiopsis in this study. Further, ITS and TEF genes appeared to be unreliable molecular markers for phylogenetic investigation. Concatenated approach between both genes (ITS and TEF) yielded many polytomies and resulted in low bootstrap support even for isolates from the same phylogenetic species. Therefore, the weak phylogenetic signal is substantially reinforced when incongruent datasets are concatenated (Gadagkar et al., 2005). Interestingly, both methods (BI and ML) from the combination of the three loci exhibited similar resolution and support as the TUB topologies, which were obtained from the same methods. This gain in accuracy, mainly for BI, might be due to the addition of a high informative dataset (TUB), overcoming certain systematic biases encountered in the tree topology using the combination of ITS and TEF genes.

In a previous study of Pestalotiopsis and allied genera from Camellia (Liu et al., 2017), phylogenies indicate a narrow relationship among morphological groupings. However, in this work, conidial features overlapped and they were not suitable for differentiating taxa or delimiting morphological species boundaries. Maharachchikumbura et al. (2012) and Solarte et al. (2018) also encountered challenges in separating isolates, especially those with plastic and variable traits. In accordance with their studies, this situation made it necessary to use phylogenetic analysis to better understand species delimitation.

The isolates COAD 2464, COAD 2465, COAD 2466, and COAD 2395 clustered together and formed a distinct clade (0.9 for BI) from the subclades N. javaensis, N. mesopotamica, and N. rosae. However, we did not regard them as a novel species since the specimens differ from N. javaensis, N. foedans, N. mesopotamica, and N. rosae ex-

types in only five, eight, nine, and five base pairs (bp), respectively, in sequenced loci. In addition, those isolates have indistinguishable morphological characters among other isolates belonging to different species. Considering that our objective was phytopathological rather than taxonomic, further studies could be conducted to gain insights into more informative loci, such as RPB1 and RPB2, that might improve inferences and provide better separation of phylogenetic species.

Lastly, considering the importance of Neopestalotiopsis spp. on aerial parts of eucalyptus, comprehension of the favorable conditions required for disease progress may provide a basis for developing novel management strategies in forest nurseries.

ACKNOWLEDGEMENTS

We thank MSc Vanessa Pereira de Abreu, MSc Caroline Hawerroth, and Dr. Fabrício de Ávila Rodrigues for their assistance; Dr. Henrique Duarte for valuable advice on data analysis. This study was financially supported by Cellulose Nipo-Brasileira (CENIBRA) and the Brazilian National Council for Scientific and Technological Development (CNPq).

REFERENCES

ABRAF – Associação Brasileira de Produtores de Florestas Plantadas, 2013. Anuário estatístico 2013. ABRAF, Brasília.

Akinsanmi O.A., Nisa S., Jeff-Ego O.S., Shivas R.G., Drenth A., 2017. Dry flower disease of Macadamia in Australia caused by Neopestalotiopsis macadamiae sp. nov. and Pestalotiopsis macadamiae sp. nov. Plant Dis. 1, 45–53.

Alfenas, A.C., Zauza E.A.V., Mafia, R.G., Assis, T.F., 2009. Clonagem e Doenças do Eucalipto, second ed. UFV, Viçosa.

ANPSA – Australian Native Plants Society, 2017. The Eucalypts. http://anpsa.org.au/eucalypt.html (accessed 29 November 2017).

Bezerra J.D.P., Machado A.R., Firmino A.L., Rosado A.W.C., Souza C.A.F., Souza-Motta C.M., Freire K.T.L.S., Paiva L.M., Magalhães O.M.C., Pereira O.L., Crous P.W., Oliveira T.G.L., Abreu V.P., Fan X., 2018. Mycological Diversity Description I. Acta Bot. Bras. 1, 1–11.

Brown, B.N., Ferreira, F.A., 2000. Diseases during propagation of eucalypts, in: Keane, P.J., Kile, G.A., Podger, F.D., Brown, B.N. (Eds.), Diseases and Pathogens of Eucalypts. CSIRO Publish, Collingwood, pp. 119–151.

Carbone I., Kohn L.M., 1999. A method for designing primer sets for speciation studies in filamentous ascomycetes. Mycologia. 91, 553–556.

Carroll J.E., Wilcox W.F., 2003. Effects of humidity on the development of grapevine powdery mildew. Phytopathology. 93, 1137–1144.

Chen S., Wyk M.V., Roux J., Wingfield M.J., Xie Y., Zhou X., 2013. Taxonomy and pathogenicity of Ceratocystis species on eucalyptus trees in South China, including C. chinaeucensis sp. nov. Fung. Div. 58, 267–279.

Corel Inc., 2018. CorelDRAW Graphics Suite 2018. https://www.coreldraw.com/br/ (accessed 03 June 2018).

Coyier, D.L., Roane, M.K., 1986. Compendium of Rhododendron and Azalea Diseases. The American Phytopathological Society (APS) Press, St. Paul.

Crous P.W., Summerell B.A., Swart L., Denman S., Taylor J.E., Bezuidenhout C.M., Palm M.E., Marincowitz S., Groenewald J.Z., 2011. Fungal pathogens of Proteaceae. Persoonia. 27, 20–45.

Crous P.W. et al., 2015. Fungal planet description sheets: 371–399. Persoonia. 35, 264–327.

Darriba D., Taboada G.L., Doallo R., Posada D., 2012. jModelTest 2: more models, new heuristics and parallel computing. Nat. Methods. 9, 772.

Das R., Chutia M., Das K., Jha D.K, 2010. Factors affecting sporulation of Pestalotiopsis disseminata causing grey blight disease of Persea bombycina Kost., the primary food plant of muga silkworm. Crop. Prot. 29, 963–968.

El-Argawy E., 2015. Characterization and control of Pestalotiopsis spp. the causal fungus of guava scabby canker in El-Beheira Governorate, Egypt. Int. J. Phytopathol. 4, 121–136.

Elmer W.H., Ferrandino F.J., 1995. Influence of spore density, leaf age, temperature, and dew periods on septoria leaf spot of tomato. Plant Dis. 79, 287–293.

Espinoza J.G., Briceño E.X., Keith L.M., Latorre B.A., 2008. Canker and twig dieback of blueberry caused by Pestalotiopsis spp. and a Truncatella sp. in Chile. Plant Dis. 92, 1407–1414.

Ferreira, F.A., 1989. Patologia Florestal: Principais Doenças Florestais no Brasil. SIF, Viçosa.

Ferreira E., Cavalcanti P., Nogueira D., 2014. ExpDes: an R package for ANOVA and experimental designs. Applied Mathematics. 5, 2952–2958.

Gadagkar S.R., Rosenberg M.S., Kumar S., 2005. Inferring species phylogenies from multiple genes: concatenated sequence tree versus consensus gene tree. J. Exp. Zool. B. Mol. Dev. Evol. 304, 64–74.

Gevens A.J., Carver T.L.W., Thomas B.J., Nicholson R.L., 2001. Visualization and partial characterization of the ECM of Pestalotia malicola on artificial and natural substrata. Physiol. Mol. Plant Pathol. 58, 77–285.

Gilet T., Bourouiba L., 2015. Fluid fragmentation shapes rain-induced foliar disease transmission. J. R. Soc. Interface. 12.

Glass N.L., Donaldson G.C., 1995. Development of primer sets designed for use with the PCR to amplify conserved genes from filamentous ascomycetes. Appl. Environ. Microbiol. 61, 1323–1330.

Hepperle D., 2004. SeqAssem: a sequence analysis tool, contig assembler and trace data visualization tool for molecular sequences. http://www.sequentix.de (accessed 01 February 2018).

Hopkins K.E., McQuilken M.P., 2000. Characteristics of Pestalotiopsis associated with hardy ornamental plants in the UK. Eur. J. Plant Pathol. 106, 77–85.

Hu H., Jeewon R., Zhou D., Zhou T., Hyde K.D., 2007. Phylogenetic diversity of endophytic Pestalotiopsis species in Pinus armandii and Ribes spp.: evidence from rDNA and β-tubulin gene phylogenies. Fung. Div. 24, 1–22.

Huber L., Gillespie T. J., 1992. Modeling leaf wetness in relation to plant disease epidemiology. Annu. Rev. Phytopathol. 30, 553–577.

Hyde K.D., Nilsson R.H., Alias S.A., Ariyawansa H.A., Blair J.E., Cai L., Cock A.W.A.M., Dissanayake A.J., Glockling S.L., Goonasekara I.D., Gorczak M., Hahn M., Jayawardena R.S., Kan J.A.L., Laurence M.H., 2014. One stop shop: backbones trees for important phytopathogenic genera: I. Fung. Div. 67, 1–105.

Ibá (Indústria Brasileira de Árvores), 2017. Relatório Ibá 2017. http://iba.org/images/shared/Biblioteca/IBA_RelatorioAnual2017.pdf (accessed 05 November 2017).

Jeewon R., Liew E.C.Y., Hyde K.D., 2004. Phylogenetic evaluation of species nomenclature of Pestalotiopsis in relation to host association. Fung. Div. 17, 39–55.

Katerji N., Hallaire M., Menoux-Boyer Y., Durand, B., 1986. Modelling diurnal patterns of leaf water potential in field conditions. Ecol. Model. 33, 185–203.

Keith L.M., Velasquez M.E., Zee F.T., 2006. Identification and characterization of Pestalotiopsis spp. causing scab disease of guava, Psidium guajava, in Hawaii. Plant Dis. 90, 16–23.

Kitajima, E.W., Leite, B., 1999. Curso Introdutório de Microscopia Eletrônica de Varredura, second ed. ESALQ/USP, Piracicaba.

Kumar S., Stecher G., Tamura K. 2016. MEGA7: molecular evolutionary genetics analysis version 7.0 for bigger datasets. Mol. Biol. Evol. 33, 1870–1874.

Larkin M.A., Blackshields G., Brown N.P., Chenna R., McGettigan P.A., McWilliam H., Valentin F., Wallace I.M., Wilm A., Lopez R., Thompson J.D., Gibson T.J., Higgins D.G., 2007. Clustal W and Clustal X version 2.0. Bioinformatics. 23, 2947–2948.

Lazarotto M., Bovolini M.P., Muniz M.F.B., Harakawa R., Reiniger L.R.S., Santos A.F., 2014. Identification and characterization of pathogenic Pestalotiopsis species to pecan tree in Brazil. Pesq. Agropec. Bras. 49, 440–448.

Liu F., Hou L., Raza M., Cai L., 2017. Pestalotiopsis and allied genera from Camellia, with description of 11 new species from China. Sci. Rep. 7, 2045–2322.

Madar Z., Solel Z., Kimchi M., 1991. Pestalotiopsis canker of cypress in Israel. Phytoparasitica. 19, 79–81.

Maharachchikumbura S.S.N., Guo L.D., Chukeatirote E., Bahkali A.H., Hyde K.D., 2011. Pestalotiopsis – morphology, phylogeny, biochemistry and diversity. Fung. Div. 50, 167–187.

Maharachchikumbura S.S.N., Guo L.D., Cai L., 2012. A multi-locus backbone tree for Pestalotiopsis, with a polyphasic characterization of 14 new species. Fung. Div. 56, 95–129.

Maharachchikumbura S.S.N., Hyde K.D., Groenewald J.Z., Xu J., Crous P.W., 2014. Pestalotiopsis revisited. Stud. Mycol. 79, 121–186.

Maharachchikumbura S.S.N., Hyde K.D., Jones E.B.G., McKenzie E.H.C., 2016. Families of Sordariomycetes. Fung. Div. 79, 1–317.

Miller, M.A., Pfeiffer, W., Schwartz, T., 2010. Creating the CIPRES Science Gateway for inference of large phylogenetic trees, in: Proceedings of the Gateway Computing Environments Workshop (GCE), New Orleans, pp. 1–8.

Minitab Inc., 2010. Minitab 17 Statistical Software. http://minitab.com (accessed 06 March 2018).

Mittal, R.K., Anderson, R.L., Mathur, S.B., 1990. Microorganisms associated with tree seeds: world checklist 1990: Information Report PI-X-96. Petawawa National Forestry Institute, Ontario.

Myleus Biotecnologia, 2018. Sequenciamento de DNA: serviço de sequenciamento de DNA por eletroforese capilar - método de Sanger. http://facility.myleus.com/ (accessed 07 February 2018).

O'Donnell K., Cigelnik E., 1997. Two divergent intragenomic rDNA ITS2 types within a monophyletic lineage of the fungus Fusarium are nonorthologous. Mol. Phylogenet. Evol. 7, 103–116.

O'Donnell K., Kistler H.C., Cigelnik E., Ploetz R.C., 1998. Multiple evolutionary origins of the fungus causing panama disease of banana: concordant evidence from nuclear and mitochondrial gene genealogies. Proc. Natl. Acad. Sci. SA (PNAS). 98, 2044–2049.

Oliveira, J.A., 1991. Efeito do Tratamento Fungicida em Sementes no Controle de Tombamento de Plântulas de Pepino (Cucumis sativus L.) e Pimentão (Capsicum annuum L.). Escola Superior de Agricultura de Lavras, Lavras.

Pinho D.B., Firmino A.L., Ferreira-Junior W.G., Pereira O.L., 2013. An efficient protocol for DNA extraction from Meliolales and the description of Meliola centellae sp. nov. Mycotaxon. 122, 333–345.

Pirone, P.P., 1978. Diseases and Pests of Ornamental Plants. Wiley Interscience, New York.

Rambaut A., 2009. FigTree 1.2.2. http://tree.bio.ed.ac.uk/so ftware/figtree/ (accessed 10 February 2018).

Rayner, R.W., 1970. A Mycological Colour Chart. Commonwealth Mycological Institute (CMI), Kew.

Rodrigues F.A., Silva I.T., Cruz M.F.A, Carré-Missio V., 2014. The Infection process of Pestalotiopsis longisetula leaf spot on strawberry leaves. J. Phytopathol. 162, 690–692.

Ronquist F., Huelsenbeck J.P., 2003. MrBayes 3: Bayesian phylogenetic inference under mixed models. Bioinformatics. 19, 1572–1574.

Rosado A.W.C., Machado, A.R., Pereira O.L., 2015. Postharvest stem-end rot on immature coconut caused by Pestalotiopsis adusta in Brazil. Plant Dis. 99, 1036–1036.

Schuh W., 1991. Influence of temperature and leaf wetness period on conidial germination in vitro and infection of Cercospora kikuchii on soybean. Phytopathology. 81, 1315–1318.

Silva H.R., Pozza E.A., Souza P.E., Ferreira M.A., Freitas A.S., Moreira S.I., 2018. Cercospora leaf spot in Toona ciliata: epidemiology and infection process of Cercospora cf. alchemillicola. For. Pathol; e12451.

Solarte F., Muñoz C.G., Maharachchikumbura S.S.N., Álvarez E. 2018. Diversity of Neopestalotiopsis and Pestalotiopsis spp., causal agents of guava scab in Colombia. 102.

Sutton, B.C., 1980. The Coelomycetes: Fungi Imperfecti with Pycnidia, Acervuli and Stromata, illustrated ed. Commonwealth Mycological Institute (CMI), Kew.

Systat Software Inc., 2018. SigmaPlot version 11. http://www.sigmaplot.co.uk (accessed 28 May 2018).

Tagne A., Mathur S.B., 2001. First report of chlorotic spot of maize caused by Pestalotiopsis neglecta. New Dis. Rep. 50, 791–791.

Watanabe K., Motohashi K., Ono Y., 2010. Description of Pestalotiopsis pallidotheae: a new species from Japan. Mycoscience. 51, 182–188.

White, T.J., Bruns, T., Lee, S., Taylor, J., 1990. Amplification and direct sequencing of fungal ribosomal RNA genes for phylogenetics, in: Innis, M.A., Gelfand, D.H., Sninsky,

J.J., White, T.J. (Eds.), PCR Protocols a Guide to Methods and Applications. Academic Press, London, pp. 315–322.

Yuan Z.Q., Mohammed C., 1997. Investigation of fungi associated with stem cankers of eucalypts in Tasmania, Australia. Aust. Plant Pathol. 26, 78–84.

Zaldúa S., Sanfuentes E., 2010. Control of Botrytis cinerea in Eucalyptus globulus mini-cuttings using Clonostachys and Trichoderma strains. Chil. J. Agric. Res. 70, 576–582.

Zauza, E.A.V., Alfenas, A.C., Mafia, R.G., 2007. Esterilização, preparo de meios de cultura e fatores associados ao cultivo de fitopatógenos, in: Alfenas, A.C., Mafia, R.G. (Eds.), Métodos em Fitopatologia. UFV, Viçosa, pp. 23–51.

Zeng W., Melotto M., He S.Y., 2010. Plant stomata: a checkpoint of host immunity and pathogen virulence. Curr. Opin. Biotechnol. 21, 599–603.

TABLES AND FIGURES

Table 1. GenBank accession numbers of DNA sequences of Neopestalotiopsis species used in the phylogenetic analyses.

Species	Isolates	Genbank Accession nº			Host	Country	Reference
		ITS	TUB	TEF			
Neopestalotiopsis aotearoa	CBS 367.54	KM199369	KM199454	KM199526	Canvas	New Zealand	Maharachchikumbura et al., 2014
N. asiatica	MFLUCC 12-0286	JX398983	JX399018	JX399049	Unidentified tree	China	Maharachchikumbura et al., 2014
N. australis	CBS 114159	KM199348	KM199432	KM199537	Telopea sp.	Australia	Maharachchikumbura et al., 2014
N. brasiliensis	COAD 2166	MG686469	MG692400	MG692402	Psidium guajava	Brazil	Bezerra et al., 2018
N. chrysea	MFLUCC 12-0261	JX398985	JX399020	JX399051	Dead leaves	China	Maharachchikumbura et al., 2014
N. chrysea	MFLUCC 12-0262	JX398986	JX399021	JX399052	Dead plant	China	Maharachchikumbura et al., 2014
N. clavispora	MFLUCC 12-0280	JX398978	JX399013	JX399044	Magnolia sp.	China	Maharachchikumbura et al., 2014
N. clavispora	MFLUCC 12-0281	JX398979	JX399014	JX399045	Magnolia sp.	China	Maharachchikumbura et al., 2014
N. cubana	CBS 600.96	KM199347	KM199438	KM199521	Leaf litter	Cuba	Maharachchikumbura et al., 2014
N. ellipsospora	MFLUCC 12-0283	JX398980	JX399016	JX399047	Dead plant materials	China	Maharachchikumbura et al., 2014
N. ellipsospora	MFLUCC 12-0284	JX398981	JX399015	JX399046	Dead plant materials	Thailand	Maharachchikumbura et al., 2014
N. egyptiaca	CBS 140162	KP943747	KP943746	KP943748	Mangifera indica	Egypt	Crous et al., 2015
N. egyptiaca	COAD 2167	MG686470	MG692401	MG692403	Psidium guajava	Brazil	Bezerra et al., 2018
N. eucalypticola	CBS 264.37	KM199376	KM199431	KM199551	Eucalyptus globulus	—	Maharachchikumbura et al., 2014
N. foedans	CGMCC 3.9123	JX398987	JX399022	JX399053	Rhizophora mangle	China	Maharachchikumbura et al., 2012
N. foedans	CGMCC 3.9202	JX398988	JX399023	JX399054	Calliandra haematocephala	China	Maharachchikumbura et al., 2012
N. formicarum	CBS 115.83	KM199344	KM199444	KM199519	Plant debris	Cuba	Maharachchikumbura et al., 2014
N. formicarum	CBS 362.72	KM199358	KM199455	KM199517	Dead Formicidae (ant)	Ghana	Maharachchikumbura et al., 2014

N. honoluluana	CBS 111535	KM199363	KM199461	KM199546	Telopea sp.	USA	Maharachchikumbura et al., 2014
N. honoluluana	CBS 114495	KM199364	KM199457	KM199548	Telopea sp.	USA	Maharachchikumbura et al., 2014
N. javaensis	CBS 257.31	KM199357	KM199437	KM199543	Cocos nucifera	Indonesia	Maharachchikumbura et al., 2014
N. macadamiae	BRIP 63737c	KX186604	KX186654	KX186627	Macadamia integrifolia	Australia	Akinsanmi et al., 2017
N. mesopotamica	CBS 299.74	KM199361	KM199435	KM199541	Eucalyptus sp.	Turkey	Maharachchikumbura et al., 2014
N. mesopotamica	CBS 336.86	KM199362	KM199441	KM199555	Pinus brutia	Iraq	Maharachchikumbura et al., 2014
N. piceana	CBS 254.32	KM199372	KM199452	KM199529	Cocos nucifera	Indonesia	Maharachchikumbura et al., 2014
N. piceana	CBS 394.48	KM199368	KM199453	KM199527	Picea sp.	UK	Maharachchikumbura et al., 2014
N. protearum	CBS 114178	JN712498	KM199463	KM199542	Leucospermum cuneiforme cv. 'Sunbird'	Zimbabwe	Crous et al., 2011
N. rosae	CBS 124745	KM199360	KM199430	KM199524	Paeonia suffruticosa	USA	Maharachchikumbura et al., 2014
N. rosae	CBS 101057	KM199359	KM199429	KM199523	Rosa sp.	New Zealand	Maharachchikumbura et al., 2014
N. samarangensis	CBS 115451	KM199365	KM199447	KM199556	Unidentified tree	Hong Kong	Maharachchikumbura et al., 2014
N. samarangensis	MFLUCC 12-0233	JQ968609	JQ968610	JQ968611	Syzygium samarangense	Thailand	Maharachchikumbura et al., 2014
N. saprophytica	CBS 115452	KM199345	KM199433	KM199538	Litsea rotundifolia	Hong Kong	Maharachchikumbura et al., 2014
N. saprophytica	MFLUCC 12-0282	JX398982	JX399017	JX399048	Magnolia sp.	China	Maharachchikumbura et al., 2014
N. sp. 4	CBS 233.79	KM199373	KM199464	KM199528	Crotalaria juncea	India	Maharachchikumbura et al., 2014
N. sp. 10	CBS 110.20	KM199342	KM199442	KM199540	—	—	Maharachchikumbura et al., 2014
N. sp. 15	CBS 177.25	KM199370	KM199445	KM199533	Dalbergia sp.	—	Maharachchikumbura et al., 2014
N. sp. 15	CBS 664.94	KM199354	KM199449	KM199525	Cocos nucifera	Netherlands	Maharachchikumbura et al., 2014
N. sp. 20	CBS 164.42	KM199367	KM199434	KM199520	Dune sand	France	Maharachchikumbura et al., 2014
N. sp. 20	CBS 360.61	KM199346	KM199440	KM199522	Cinchona sp.	Guinea	Maharachchikumbura et al., 2014
N. sp. 22	CBS 119.75	KM199356	KM199439	KM199531	Achras sapota	India	Maharachchikumbura et al., 2014
N. sp. 26	CBS 266.37	KM199349	KM199459	KM199547	Erica sp.	Germany	Maharachchikumbura et al., 2014
N. sp. 26	CBS 361.61	KM199355	KM199460	KM199549	Cissus sp.	Netherlands	Maharachchikumbura et al., 2014
N. surinamensis	CBS 450.74	KM199351	KM199465	KM199518	Soil under Elaeis guineensis	Suriname	Maharachchikumbura et al., 2014

N. surinamensis	CBS 111494	JX556232	KM199462	KM199530	Protea eximia	Zimbabwe	Maharachchikumbura et al., 2014
N. umbrinospora	MFLUCC 12-0285	JX398984	JX399019	JX399050	Unidentified plant	China	Maharachchikumbura et al., 2014
Pseudopestalotiopsis theae	MFLUCC 12-0055	JQ683727	JQ683711	JQ683743	Camellia sinensis	Thailand	Maharachchikumbura et al., 2014
N. rosae*	**COAD 2392**	XXXXXX	XXXXXX	XXXXXX	Eucalyptus CNB 019	Brazil	This study
N. protearum*	**COAD 2393**	XXXXXX	XXXXXX	XXXXXX	Eucalyptus CNB 019	Brazil	This study
N. protearum*	**COAD 2394**	XXXXXX	XXXXXX	XXXXXX	Eucalyptus CNB 019	Brazil	This study
N. sp.*	**COAD 2395**	XXXXXX	XXXXXX	XXXXXX	Eucalyptus CNB 019	Brazil	This study
N. sp.*	**COAD 2464**	XXXXXX	XXXXXX	XXXXXX	Eucalyptus CNB 019	Brazil	This study
N. sp.*	**COAD 2465**	XXXXXX	XXXXXX	XXXXXX	Eucalyptus CNB 019	Brazil	This study
N. sp.*	**COAD 2466**	XXXXXX	XXXXXX	XXXXXX	Eucalyptus CNB 019	Brazil	This study
N. rosae*	**COAD 2467**	XXXXXX	XXXXXX	XXXXXX	Eucalyptus CNB 019	Brazil	This study

*Isolates obtained in this study. Ex-types are highlighted in bold.

Table 2. Isolates of Neopestalotiopsis spp. obtained from different host species of Myrtaceae and Arecaceae used in cross-inoculation tests.

ISOLATE CODE	ORIGINAL HOST	FAMILY	ISOLATE SPECIES
COAD 2017	Dypsis madagascariensis (lucuba palm)	Arecaceae	N. arecacearum
COAD 2018	Licuala grandis (ruffled fan palm)	Arecaceae	N. foedans
COAD 2020	Phoenix roebelenii (pygmy date palm)	Arecaceae	N. phoenicis
COAD 2022	Wodyetia bifurcata (foxtail palm)	Arecaceae	N. surinamensis
COAD 2166	Psidium guajava (guava)	Myrtaceae	N. brasiliensis
COAD 2167	Psidium guajava (guava)	Myrtaceae	N. egyptiaca
COAD 2582	Caryota mitis (fishtail palm)	Arecaceae	N. caryotae
COAD 2583	Dypsis lutescens (bamboo palm)	Arecaceae	N. dypsae

Table 3. Morphological comparison between Neopestalotiopsis isolates obtained in this study.

CONIDIA				APPENDAGES	
ISOLATE	**SHAPE**	**LENGTH (µm)**	**WIDTH (µm)**	**APICAL**	**BASAL**
COAD 2392	Fusiform, straight to slightly curved	18.0 ± 1.7	6.0 ± 0.7	2–3 (often 3), tubular, 12.0–19.0 µm long, inserted at a different locus in the upper half of the apical cell	3.5 ± 0.9 µm long, tubular, centric
COAD 2393	Fusiform, straight to slightly curved	24.5 ± 2.4	7.5 ± 0.9	2–3 (often 3), tubular, unbranched 8.5–22.0 µm long	3.5 ± 0.9 µm long, filiform, centric
COAD 2394	Fusiform, straight to slightly curved	21.5 ± 1.8	6.5 ± 0.8	2–3 (often 3), tubular, unbranched 8.0–22.0 µm long	4.0 ± 0.8 µm long, filiform, centric
COAD 2395	Fusiform to ellipsoid, straight to slightly curved	21.0 ± 2.9	6.0 ± 0.8	2–3, tubular, unbranched 10.0–25.5 µm long	3.5 ± 0.9 µm long, tubular to filiform, centric
COAD 2464	Fusiform to ellipsoid, straight to slightly curved	24.0 ± 2.8	6.0 ± 0.7	2-3 (often 3), tubular, unbranched 9.5–17.0 µm long	4.0 ± 1.4 µm long, single, tubular to filiform, centric
COAD 2465	Fusiform to ellipsoid, straight to slightly curved	22.5 ± 2.1	6.0 ± 0.7	2–3, tubular, unbranched 9.5–19.0 µm long	5.0 ± 0.9 µm long, single, tubular to filiform, centric
COAD 2466	Fusiform to ellipsoid, straight to slightly curved	24.0 ± 2.4	6.5 ± 0.6	2–3 (often 3), tubular, unbranched 10.0–18.5 µm long	5.0 ± 1.1 µm long, single, tubular to filiform, centric
COAD 2467	Fusiform, straight to slightly curved	24.5 ± 2.7	7.0 ± 0.7	2–3 (often 3), tubular, 13.0–22.0 µm long, inserted at a different locus in the upper half of the apical cell	4.0 ± 1.4 µm long, tubular, centric

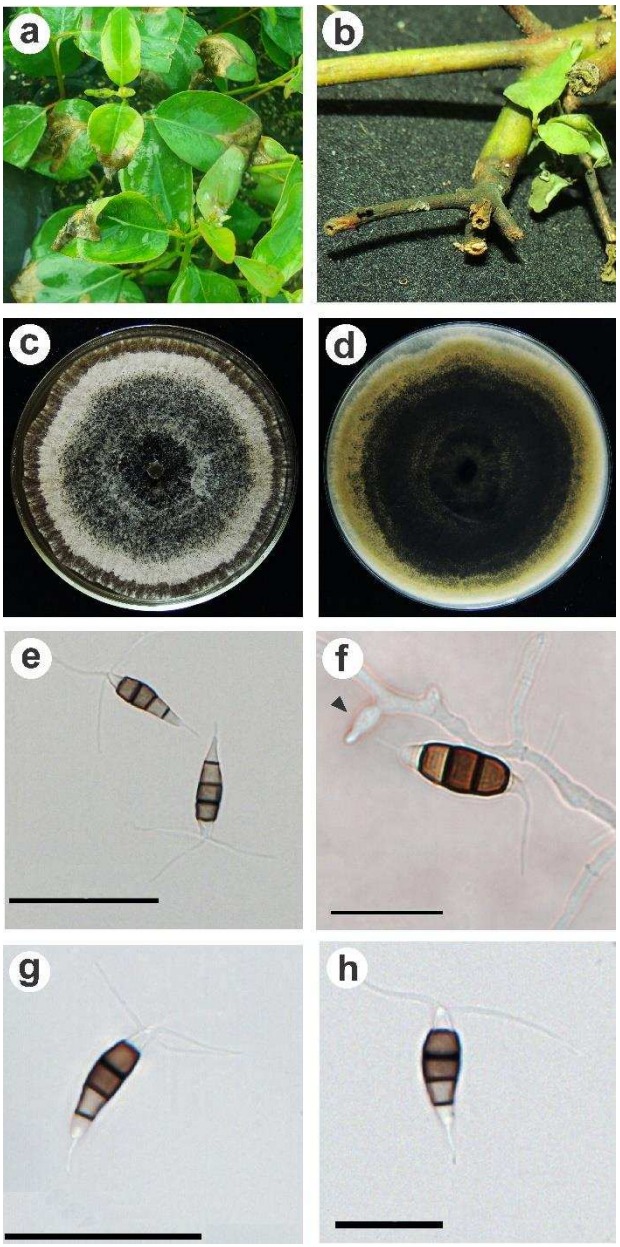

Figure 1. Neopestalotiopsis spp. on Eucalyptus grandis×Eucalyptus urophylla. **(a)** Pestalotiopsis leaf spot symptoms observed on eucalyptus mini-cuttings' leaves in the forest nursery. **(b)** Stem lesions on eucalyptus seedlings in detail. **(c)** Upper surface view of the 8-day-old culture grown on potato dextrose agar (PDA). **(d)** Reverse view of the 8-day-old culture grown on PDA. **(e)** Conidiogenous cells and conidia of N. protearum. **(f)** Conidia of N. sp. **(g–h)** Conidia of N. rosae. Scale bars: e–h = 20 μm.

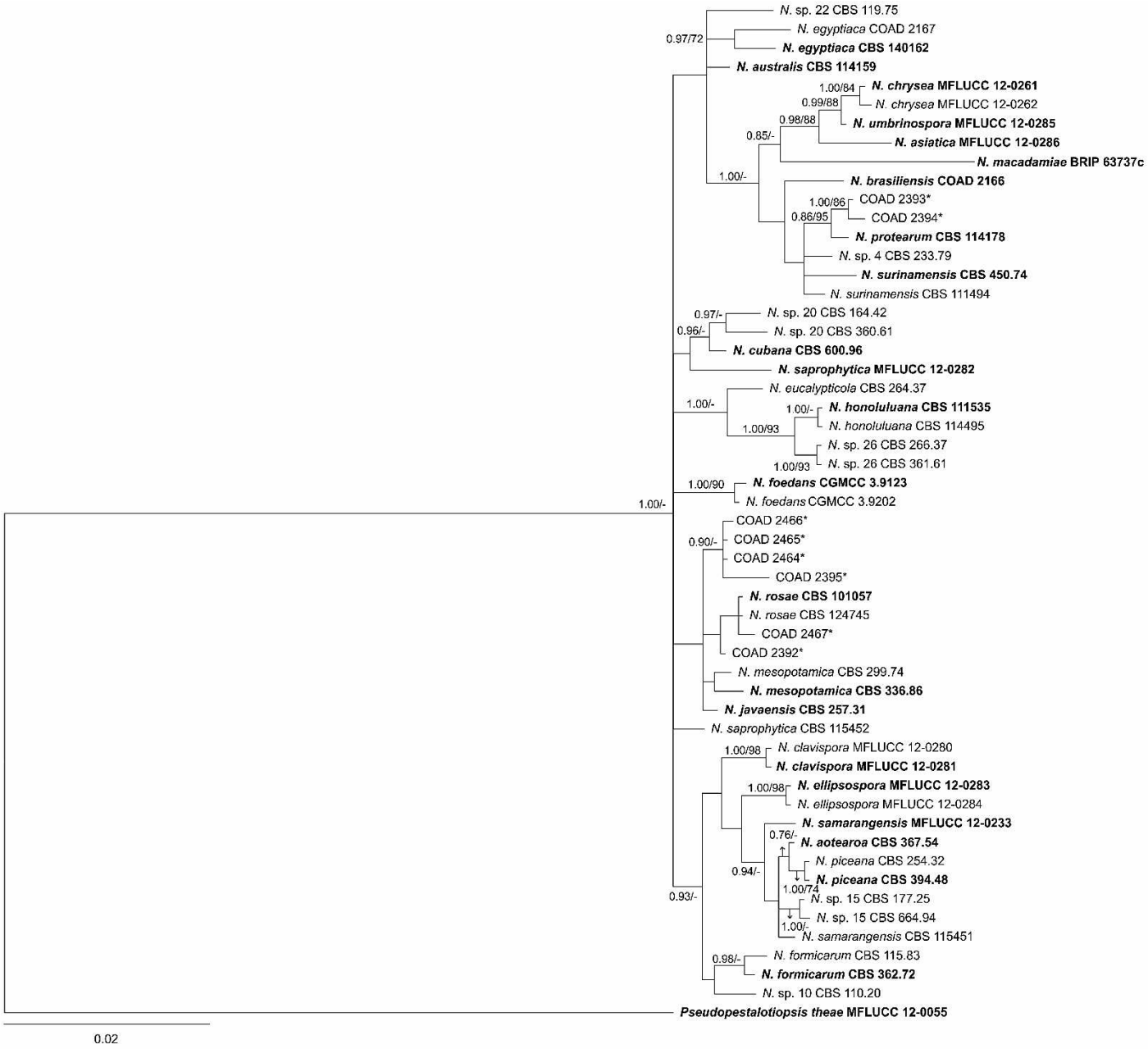

Figure 2. Multilocus phylogenetic tree based on Bayesian Inference (BI) and Maximum Likelihood (ML) using the alignment of combined sequences (ITS + TEF + TUB) of Neopestalotiopsis species. Bayesian posterior probabilities and bootstrap values for ML higher than 0.85/70 are shown respectively at the nodes (BI/ML). The tree was rooted with Pseudopestalotiopsis theae MFLUCC 12-0055. Ex-type strains are emphasized in bold. Stars (*) indicate the isolates obtained in this study.

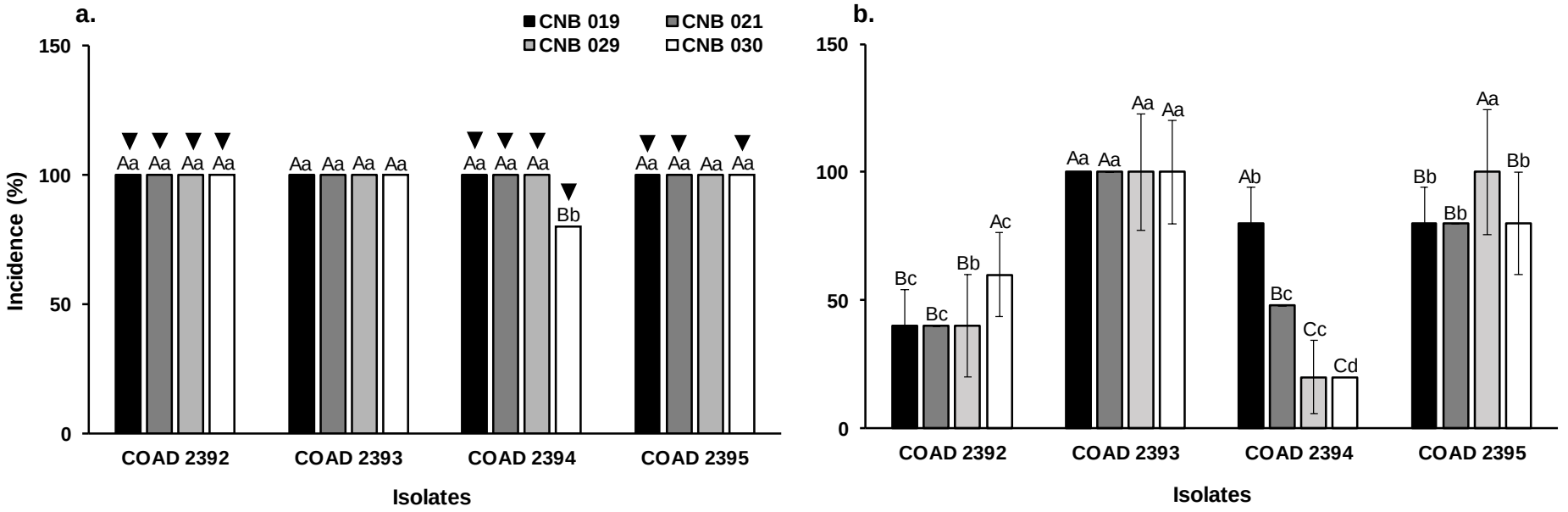

Figure 3. Pestalotiopsis leaf spot incidence (%) on commercial hybrid clones of Eucalyptus grandis×Eucalyptus urophylla (CNB 019, CNB 021, CNB 029, and CNB 030) inoculated with different fungal isolates (COAD 2392, COAD 2393, COAD 2394, and COAD 2395) with **(a)** and without leaf wounding **(b)**. Different capital letters denote significant differences among means for commercial clones and different small letters represent significant differences among means for isolates by the Tukey's test ($P \leq 0.05$). Inverted triangles denote significant differences among means for inoculation methods (wounded and unwounded leaves) by the F-test at $P \leq 0.05$. Values are means and bars represent the standard deviation of five replicates. Incidence (% leaves infected) was measured 10 days after inoculation (dai).

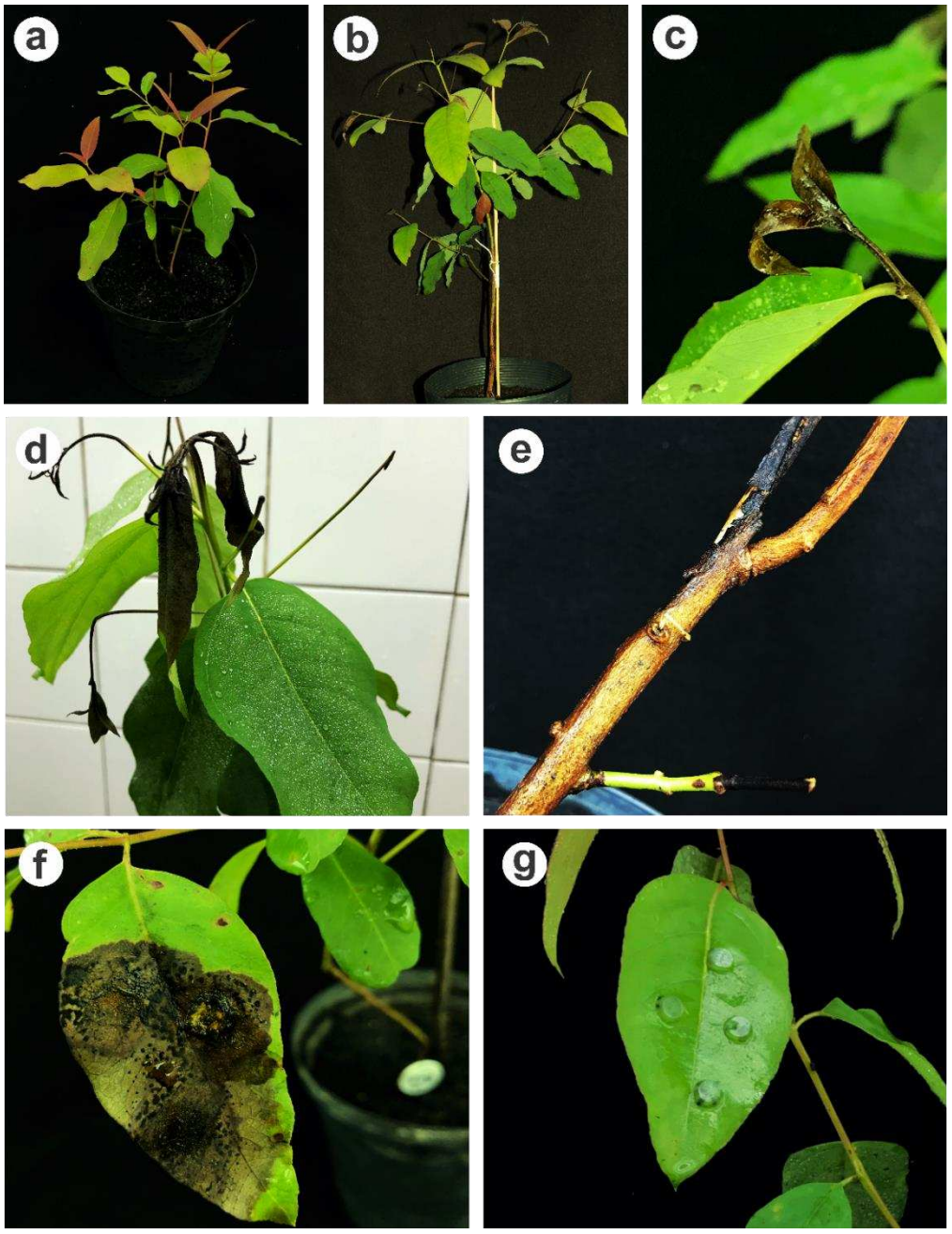

Figure 4. Effect of leaf wetness periods on the development of pestalotiopsis leaf spot **(a-e)** and pathogenicity test results **(f and g)**. **(a)** Seedling kept in a mist irrigation chamber under 24h and transferred to a growth chamber. **(b)** Seedling kept in a mist irrigation chamber under 48h and transferred to a growth chamber. **(c)** Seedling kept in a mist irrigation chamber under 72h and transferred to a growth chamber. **(d–e)** Seedlings subjected to 168h of continuous wetness. **(f)** Lesions and black conidiomata developing on the surface of wounded leaves 5 days after inoculation. **(g)** Wounded leaf inoculated with sterile PDA disks (control).

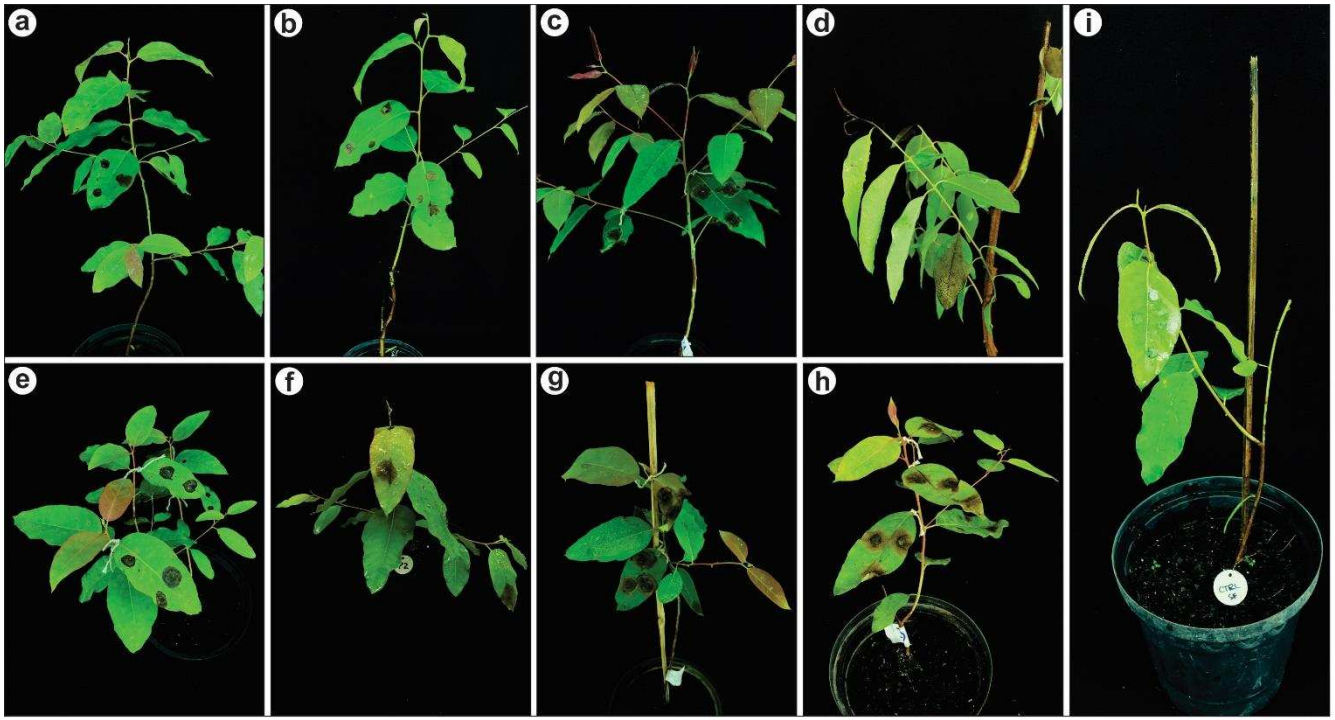

Figure 5. Inoculation tests of Neopestalotiopsis spp., originally obtained from different species of Arecaceae and Myrtaceae, on Eucalyptus grandis× Eucalyptus urophylla (CNB 019) 168 hours after inoculation (hai). Unwounded leaves were inoculated with: **(a)** Neopestalotiopsis arecacearum COAD 2017. **(b)** N. foedans COAD 2018. **(c)** N. phoenicis COAD 2020. **(d)** N. surinamensis COAD 2022. **(e)** N. brasiliensis COAD 2166. **(f)** N. egyptiaca COAD 2167. **(g)** N. caryotae COAD 2582. **(h)** N. dypsae COAD 2583. **(i)** Unwounded leaf inoculated with sterile PDA disks without mycelium (control).

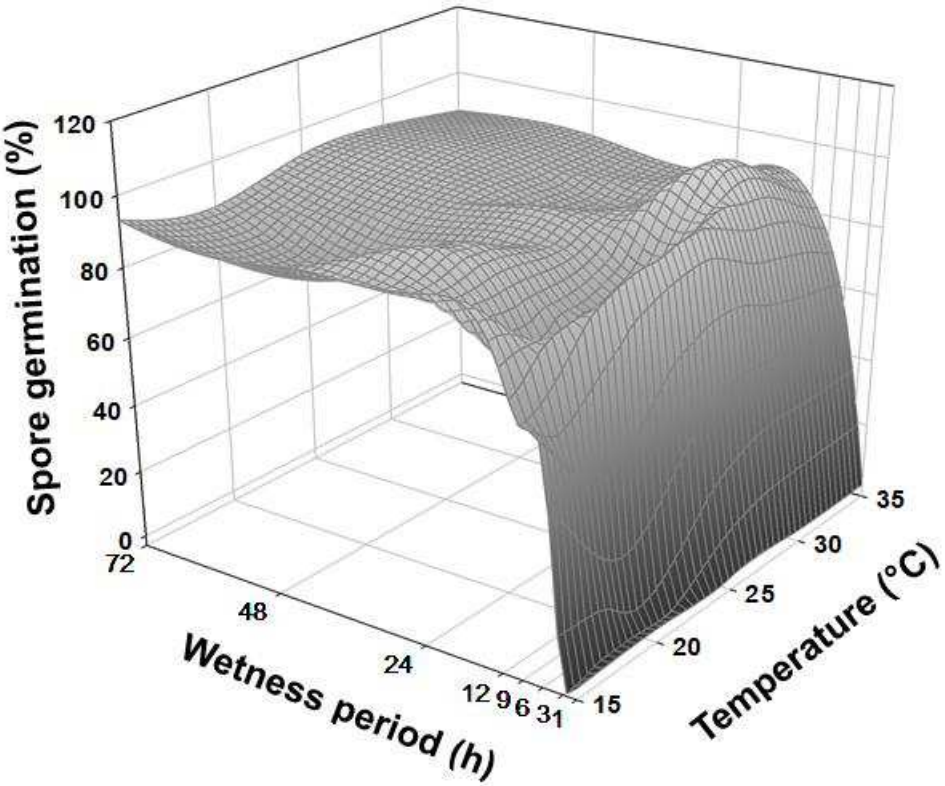

Figure 6. Effects of temperature (15, 20, 25, 30 or 35°C) and duration of wetness (1, 3, 6, 9, 12, 24, 48, and 72 hours) on conidial germination (%) of Neopestalotiopsis protearum (isolate COAD 2393) under in vitro conditions. Data were represented in a surface area plot under SigmaPlot 11.

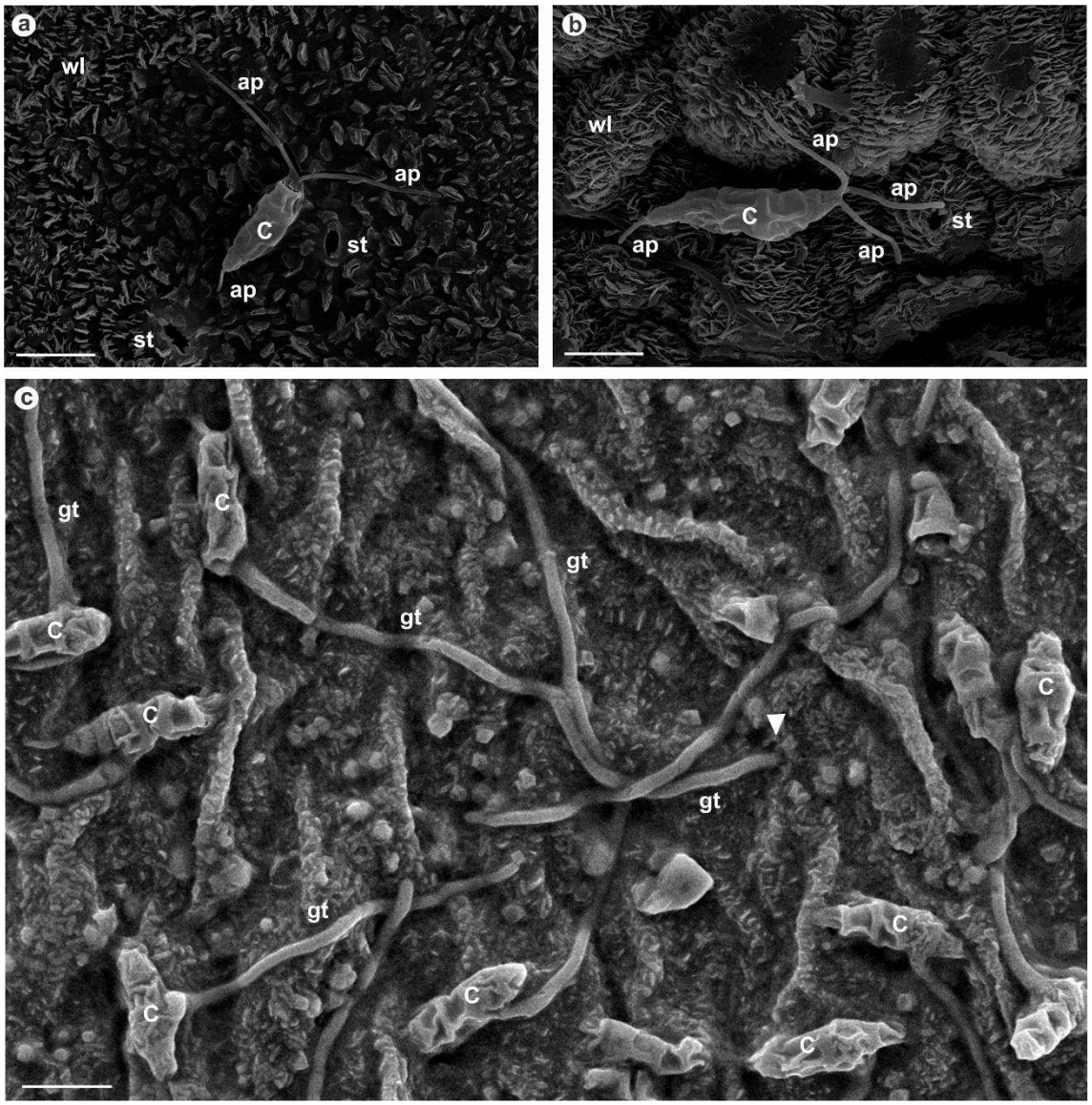

Figure 7. Scanning electron micrographs of conidial germination and penetration of Neopestalotiopsis protearum (isolate COAD 2393) on eucalyptus leaves. **(a)** Conidium preparing the site infection by secreting enzymes that degraded the wax layer on the upper surface of leaves at 3 hours after inoculation (hai), presence of one basal appendage and two apical appendages. **(b)** Conidial morphology emphasizing the presence of one basal appendage and three apical appendages, observation at 3 hai. **(c)** Conidial germination and fungal attempt to directly penetrate the epidermis of upper leaf surface at 6 hai. Bars = 10 μm. C, conidium; ap, appendage; st, stomata; wl, wax layer; gt, germ tube; arrow-head = fungal attempt to directly penetrate the epidermis.